"Science Stays True Here"
Biological and Chemical Research, 121-129 | Science Signpost Publishing

Thermodynamic and Voltammetry Investigation of Processes on the $Hg_3In_2Te_6$ Electrodes Surface

Oxana Sema, Volodymyr Diichuk, Igor Kobasa

Yu. Fedkovych National University of Chernivtsi, 2 Kotsyubynsky St., Chernivtsi, Ukraine, 580121

Received: January 21, 2017 / Accepted: February 22, 2017 / Published: May 25, 2017

Abstract: The $Hg_3In_2Te_6$ electrodes polarisation experiments at acidic, neutral and basic pH values followed by comparison of the experimental data with the results of thermodynamic calculations derived from the Pourbaix diagrams analysis have been used to identify the electrode processes occurring on the $Hg_3In_2Te_6$ surface and their products. It is proved that the mechanism of the redox processes and qualitative composition of the products formed can be predicted using both voltammetry investigation and the Pourbaix diagram analysis. These results can be useful in planning of the controlled surface modification of $Hg_3In_2Te_6$.

Key words: thermodynamic analysis, Pourbaix diagram, voltammetry diagrams, anodic polarization of $Hg_3In_2Te_6$.

1. Introduction

Investigation of the physico-chemical processes running on the semiconductor/electrolyte interphase is important to develop the surface treatment technologies and solutions required to change its properties and obtain new materials with preplanned characteristics [1-3]. This aim can reached through porosity increasing, oxidation and sulfidation of the surface by various chemical and electrochemical methods. These methods remain on the cutting edge of the modern science and technology as a powerful tool in the nanostructured modification of elementary semiconductors and complex semiconducting compounds. The semiconducting materials with modified surface, dye-sensitizers, which enable their utilization in the visible light range, and

Corresponding author: Igor Kobasa, Yu. Fedkovych National University of Chernivtsi, 2 Kotsyubynsky St., Chernivtsi, Ukraine. E-mail: i.kobasa@chnu.edu.ua.

metal doping ions are used widely in PV blocks, optoelectronic equipment, and detectors for IR and ionization irradiation [4-10].

On the other hand, building the Pourbaix diagram is another convenient tool for thermodynamic analysis and physicochemical investigation of the electrode/electrolyte interphase. Various Pourbaix diagrams of the metals[11], simple and binary semiconducting materials [12-16] are available from the references and can be used for assessment and prediction of chemical conditions of the semiconductors surface. For instance, a prediction of the chemical composition of the anodic oxide films on the surface of InSb [12] and GaAs [13] has been performed using results of E-pH diagrams analysis. Besides, same approach has been used to determine the optimal conditions for the polishing and selective etching of CdSb and CdTe monocrystals as well as a series of their solid solutions [14-16]. A thermodynamic analysis of the redox and acid-base reactions occurring in the system $Hg_2In_3Te_6 - H_2O$ at the acidic pH and potentiostatic conditions has been performed in [17] by building the Pourbaix diagram. The authors of [17] have concluded that the thermodynamic prognosis can be used as an effective tool for prognosis and evaluation of the semiconducting materials surface state.

This work has been aimed onto the complex investigation of the semiconductor/electrolyte interphase, which employed both thermodynamic analysis and polarization experiments of $Hg_2In_3Te_6$ electrodes at the acidic, neutral and basic pH and potentiostatic conditions. This investigation should clarify a possibility of the targeted influence on the physico-chemical surface processes.

2. Materials and Methods

The Pourbaix diagram for the system $Hg_3In_2Te_6$–H_2O has been developed and built in work [17] using the method of thermodynamic calculations and E-pH diagrams building method as it is described in [18, 19].

The monocrystal $Hg_3In_2Te_6$ samples with the n-type conductivity were synthesized by the Bridgeman method and used in this investigation. A thin gold film was applied chemically on the back surface of the $Hg_3In_2Te_6$ electrode and then the copper wire was soldered to the film to establish the electric contact with the crystal. The contact spot and unused surface of the electrode were isolated by picein. All electrodes were chemically etched in the polishing composition (5 % Br_2 solution in CH_3OH) and then rinsed thoroughly by bidistillate prior every measurement.

Anodic and cathodic polarization has been applied according to [20]. BAS 100B/W Electrochemical Workstation equipped with the standard three-electrode cell (Mineral glasscarbon 1.6 mm wire as a working electrode and a platinum wire as an auxiliary electrode) has been used for the cyclic voltammetry measurement of redox potentials. All the measurements were performed in the argon atmosphere at the room

temperature against silverchloride reference electrode and then transformed in the SHE scale. The working cell space was connected with reference electrode part by an electrode bridge filled with 3M NaCl solution at the reference electrode side and the working electrolyte solution – at the working cell side. These two parts of the bridge were separated by the cotton wool bead [21]. The potential scan rate was 100 mV/s.

3. Results and Discussion

The state diagram of $Hg_3In_2Te_6$–H_2O is shown in Fig. 1 for activity of the potential-determining ions $1 \cdot 10^{-6}$ mole/l.

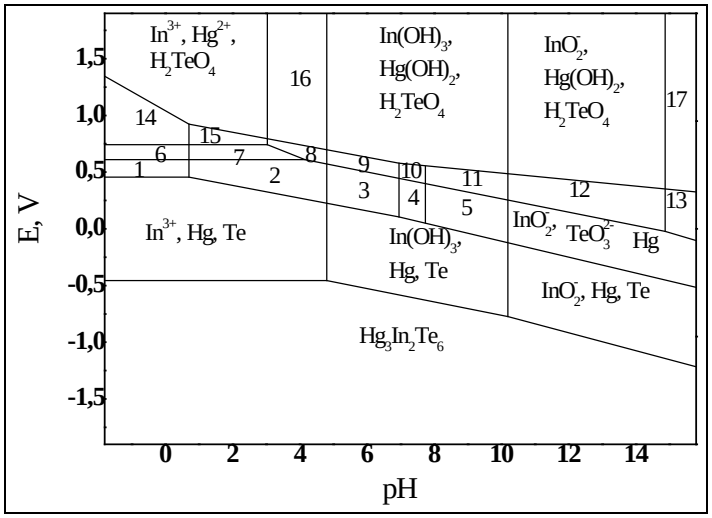

Fig. 1 The Pourbaix diagram of the system $Hg_3In_2Te_6$ (C = 10^{-6} mole/l). Areas description: (1) – In^{3+}, Hg, Te^{4+}; (2) – In^{3+}, Hg, TeO_2; (3) – $In(OH)_3$, Hg, TeO_2; (4) – $In(OH)_3$, Hg, $HTeO_3^-$; (5) – $In(OH)_3$, Hg, TeO_3^{2-}; (6) – Hg_2^{2+}, In^{3+}, Te^{4+}; (7) – Hg_2^{2+}, In^{3+}, TeO_2; (8) – $Hg(OH)_2$, In^{3+}, TeO_2; (9) – $Hg(OH)_2$, $In(OH)_3$, TeO_2; (10) – $Hg(OH)_2$, $In(OH)_3$, $HTeO_3^-$; (11) – $Hg(OH)_2$, $In(OH)_3$, TeO_3^{2-}; (12) – $Hg(OH)_2$, InO_2^-, TeO_3^{2-}; (13) – $HHgO_2^-$, InO_2^-, TeO_3^{2-}; (14) – Hg^{2+}, In^{3+}, Te^{4+}; (15) – Hg^{2+}, In^{3+}, TeO_2; (16) – In^{3+}, $Hg(OH)_2$, H_2TeO_4; (17) – $HHgO_2^-$, InO_2^-, H_2TeO_4.

The area of the solid phase $Hg_3In_2Te_6$ existence in the aqueous solutions can be derived from analysis of the diagram. This area depends on the redox potential and pH of the system and its upper boundary is limited by the polygonal line ranged between potentials -0.459 and -1.227 V. Electrode reactions that are characteristic for each fragment of this line are governed by pH, redox potential of the system and activity of the potential-determining ions.

The first fragment of the line (pH<4.8) corresponds to ionization of the most active component – indium:

$$Hg_3In_2Te_6 = 2In^{3+} + 3HgTe + 3Te + 6e^- \quad (1)$$

As a result, the semiconductor's surface gets enriched with mercury and tellurium. As seen from the diagram (Fig. 1), this enriched state of the surface remains thermodynamically stable within a wide range of potentials from -0.459 to 0.234 V. An oxidation of tellurium to Te^{4+} becomes thermodynamically allowed when the potential exceeds 0.234 V while TeO_2 can be formed for pH between 0.71 and 4.82 V (Fig. 1, areas 1 and 2). Then at the higher redox potential, the mercury oxidation reaction starts. It forms Hg_2^{2+} initially (Fig. 1, area 6) and then – Hg^{2+} (areas 14 and 15). Therefore, a stochiometric dissolution of $Hg_3In_2Te_6$ becomes thermodynamically allowed at the highly acidic pH (<0.71) and redox potentials above 0.741 V, which results in formation of the ions Hg^{2+}, In^{3+} and Te^{4+} followed by their passing into the solution. This process can be used for the polishing etching of the semiconductor surface.

The second fragment of the line is confined between the pH values 4.8 and 10.2 and it corresponds to oxidation of indium to $In(OH)_3$, which can form an amorphous phase on the surface of $Hg_3In_2Te_6$. Besides, oxidation of the surface atoms of tellurium to TeO_2 is thermodynamically allowed in the anodic region of the equilibrium potentials if pH is ranged within 4.8–6.9 (Fig. 1, area 3). Further, oxidation of Hg to $Hg(OH)_2$ becomes thermodynamically allowed if the potential exceeds 0.44 V (Fig. 1, area 9). Therefore, thermodynamic calculations prove that an oxide/hydroxide passivation film composed of TeO_2, $In(OH)_3$, $Hg(OH)_2$ and/or products of their chemical interaction can appear on the surface of $Hg_3In_2Te_6$.

Another fragment of the line (pH>12) corresponds to the selective dissolution of the In-part of $Hg_3In_2Te_6$ occurring at the potentials exceeding -0.8 V:

$$Hg_3In_2Te_6+4H_2O = 2InO_2^-+3HgTe+3Te+8H^++6e^- \quad (2)$$

Further anodic shifting of the redox potential causes initially oxidation of the surface Te atoms (when E> -0.13 V):

$$Te + 3H_2O \rightarrow TeO_3^{2-} + 6H^+ + 4e^- \quad (2.1)$$

then – oxidation of Hg (when the potential exceeds 0.24V):

$$Hg+2H_2O \rightarrow Hg(OH)_2+2H^++2e^- \quad (2.2)$$

A polarization study of $Hg_3In_2Te_6$ electrodes has been performed in acidic, basic and neutral media in order to check validity of the thermodynamic calculation prediction discussed above, and Fig. 2 represents a voltammetric curve of the sample under investigation for the acidic solution.

As seen from Fig. 2, there is an insignificant hysteresis loop in the anodic region that may be caused by some structural or chemical changes occurring to the surface of $Hg_3In_2Te_6$ monocrystals. However, another distinct hysteresis loop is present also in the cathodic region and this is the evidence of the chemical character of the changes occurring at the anodic polarization of the surface.

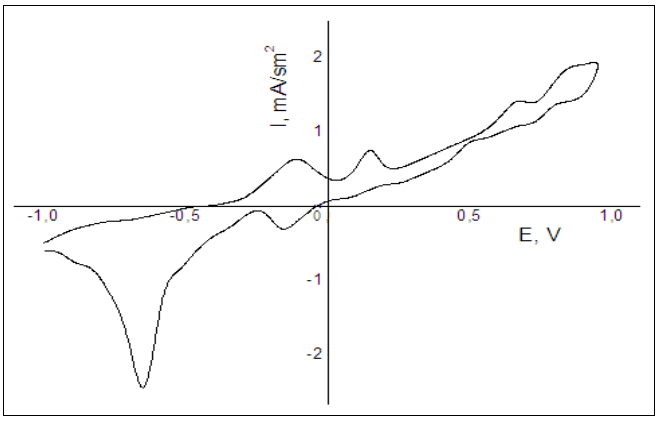

Fig. 2 Votammetric curve of $Hg_3In_2Te_6$ electrode dipped into HCl+KCl electrolyte at pH=1.9

A maximum of the cathodic current on the reverse polarization curve at -0.7 V is probably caused by cathodic reduction of the surface anodic oxidation products.

Few anodic current maximums related to the selective dissolution of the semiconductor can be seen in the curve (Fig. 2). As seen from the Pourbaix diagram, this selective dissolution is possible at the acidic pH and the electrode potential value above -0.34 V, and it results in formation of ions In^{3+} according to reaction (1).

Therefore, the first peak (E = -0.17 V) corresponds to the selective dissolution of In, which is the most active component of the semiconductor. Further decrease in the current is caused by the surface indium depletion and formation of the TeO_2 oxide film by (3) (Fig. 1, area 2):

$$Hg_3In_2Te_6+12H_2O = 2In^{3+}+3Hg+6TeO_2+24H^{+}+30e^{-} \quad (3)$$

Next maximum correspond to oxidation of Hg according to

$$Hg_3In_2Te_6+12H_2O=2In^{3+}+3Hg^{2+}+6TeO_2+24H^{+}+36e^{-} \quad (4)$$

The third peak appears at rather high potential (0.67 V) and, according to the diagram, it corresponds to the process of oxidation of TeO_2 to H_2TeO_4:

$$TeO_2+2H_2O = H_2TeO_4+2H^{+}+2e^{-} \quad (5)$$

A pattern of the voltammetry curve taken in the neutral solution is different. It exhibits only one clear anodic current maximum and the surface repassivation area. A hysteresis loop can also be noted in this system. It is especially distinct in the cathodic part of the curve and this is an evidence of the passivation films appearing on the surface of $Hg_3In_2Te_6$ monocrystal.

As seen from Fig. 3, the current value is rising until anodic polarization reaches -0.13 V and then starts to decrease because the passive and low soluble $In(OH)_3$ is accumulated on the surface. According to the thermodynamic calculations, this process is allowed in this area of negative potentials. Then the current is smoothly rising without any clear peaks at further anodic polarization from 0 to 0.8 V.

The following processes are allowed within this range according to the Pourbaix diagram (Fig. 1, areas 4 and 10):

$$Hg_3In_2Te_6+24H_2O = 3Hg + 2In(OH)_3 + 6HTeO_3 + 36H^+ + 3e^- \quad (6)$$

$$Hg_3In_2Te_6 + 30H_2O = 3Hg(OH)_2 + 2In(OH)_3 + 6HTeO_3^- + 12H^+ + 6e^- \quad (7)$$

Then the current is slightly decreasing due to formation of three low soluble compounds on the semiconductor's surface at potential 0.82 V:

$$Hg_3In_2Te_6+36H_2O = 3Hg(OH)_2 +2In(OH)_3 + 6H_2TeO_4 + 48H^+ + 48e^- \quad (8)$$

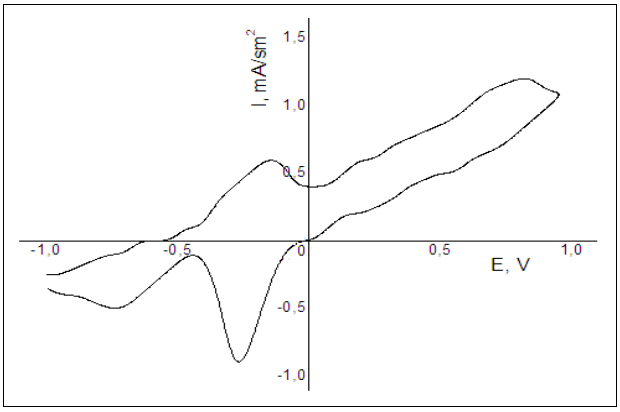

Fig. 3 Votammetric curve of $Hg_3In_2Te_6$ electrode dipped into KCl electrolyte at pH = 7

The voltammetry curve for the system under investigation in the basic media is represented in Fig. 4.

It can be seen that a small peak appears under anodic polarization at the potential -0.17 V. This peak corresponds to the selective In dissolution resulting in formation of InO_2^- ions according to reaction (2).

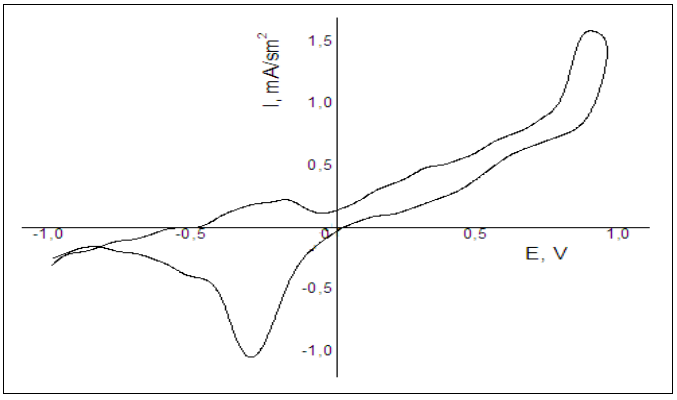

Fig. 4 Votammetric curve of $Hg_3In_2Te_6$ electrode dipped into KCl+KOH electrolyte at pH =11

An additional dissolution of the Te-component of $Hg_3In_2Te_6$ according to reactions (9) and (10) launches at further potential increase:

$$Hg_3In_2Te_6 + 22H_2O = 2InO_2^- + 6TeO_3^{2-} + 3Hg + 44H^+ + 30e^- \quad (9)$$

$$Hg_3In_2Te_6 + 28H_2O = 2InO_2^- + 6TeO_3^{2-} + 3Hg(OH)_2 + 50H^+ + 36e^- \quad (10)$$

These processes do not show any maximums in the voltammetry curve, which keeps increasing smoothly until the potential value +1.0 V when electrochemical decomposition of water results in the sharp current value jump.

4. Conclusion

As seen from the results of determination of the anolytes compositions, the thermodynamic analysis of the $Hg_3In_2Te_6$–H_2O Pourbaix diagram can be used to clarify the mechanism of the redox processes running on the semiconductor/electrolyte interphase and identify the composition of the products formed. This method can be useful in planning and optimization the conditions of electrochemical modification of $Hg_3In_2Te_6$ surface.

Besides, the conditions required for stoichiometric or selective dissolution or oxidizing of the semiconductor's surface were outlined. If the pH value is strongly acidic (<0.7) and the electrode potential is higher than 0.74 V, a stoichiometric dissolution of $Hg_3In_2Te_6$ becomes thermodynamically allowed and this process results in formation of Hg^{2+}, In^{3+} and Te^{4+} ions. When the pH is close to neutral (4,8÷6,9), and the electrode potential is over 0.44 V, a series of oxidations of the surface atoms to their oxides or hydroxides becomes possible: Te to TeO_2; Hg to $Hg(OH)_2$, and In to $In(OH)_3$. When the pH value is basic, a selective dissolution of indium and formation of InO_2^- becomes possible if the electrode potential is higher than -0.8; oxidation of the surface Te and formation of TeO_3^{2-} - if the potential is higher than -0.13 V and oxidation of Hg and formation $Hg(OH)_2$ – if the potential is higher than 0.24 V.

References

[1] Y. Li et al., "Study of barrier height and trap centers of Au/n-Hg3In2Te6 Schottky contacts by current-voltage (I-V) characteristics and deep level transient spectroscopy," J. Appl. Phys., 117, 085704 (2015).

[2] Th. Mayer et al., "Elementary processes at semiconductor/electrolyte interfaces: perspectives and limits of electron spectroscopy," Appl. Surf. Sci. 252 (1), 31-34 (2005).

[3] V.V. Diychuk, A.G. Voloshchuk, and V.V. Nechyporuk, "Electrochemical and Thermodynamic Investigation of the CdTe Single Crystals in the Na2S-NaOH-H2O Solutions," Pol. J. Chem., 83 (3), 445-454 (2009).

[4] O.G. Grushka et al., “Effect of deviations from the stoichiometric composition on the electrical and photoelectrical properties of the Hg3In2Te6 compound,” Semiconductors, 48 (10), 1271-1274 (2014).

[5] P. Gorley et.al, “Hg3In2Te6: a promising material for optoelectronic devices,” Proc. SPIE 6796, Photonics North, 67961W (2007).

[6] L.N. Kourbatov, Optoelectronics of visible and infrared spectral ranges, Fizmatkniga, Moscow, (2013).

[7] I.M.Kobasa, I.V. Kondratyeva, “Sensitizing of Semiconducting Photocatalysts by Cyanine Pigment with Two Conjugated Chromophores” Polish. J. Chem. 82(8), 1639-1648 (2008).

[8] I. Kobasa, I. Kondratyeva, and L. Odosiy, “TiO2/biscyanine and CdS/biscyanine heterostructures — Influence of the structural composition on the photocatalytic activity,” Canad. J. Chem., 88 (7), 659-666 (2010).

[9] I.M. Kobasa, “Semi-conductive materials based on the titanium dioxide doped with zinc: Catalytic activity for copper deposition and effect of UV-irradiation,” Polish J. Chem., 78 (4), 553-560 (2004).

[10] Y.S. Mazurkevich, I.M. Kobasa, “TiO2–Bi2O3 Materials Inorg. Mater., 38(5), 522–526 (2002).

[11] H.-H. Yuang “The Eh-pH Diagram and Its Advances,” Metals, 6 (1), 23 (2016) [doi:10.3390/met6010023].

[12] V.V. Yehorkin, A.P. Alehin, and S.A. Fominykh, “Application of Pourbaix Diagrams in Phase Analysis of Anodic Oxide Films on Indium Antimonide,” J. Phys. Chem., 59(8), 2085-2086 (1985).

[13] A.S. Pashinkin, et.al., “Application of Pourbaix Diagrams in Phase Analysis of Anodic Oxide Films on Gallium Arsenide,” Inorg. Mater., 27(11), 2241-2244 (1991).

[14] S.G. Dremlyuzhenko et al., “Chemical Etching of CdSb Single Crystals: Thermodynamic Analysis,” Inorg. Mater., 39(12), 1239–1245 (2003).

[15] K. Murase et al., “Potential-pH Diagram of the Cd-Te-NH3-H2O System and Electrodeposition Behavior of CdTe from Ammoniacal” Alkaline Baths,” J. Electrochem. Soc., 146 (5), 1798-1803 (1999).

[16] S.G. Dremlyuzhenko et ai., “State of Cd1-xZnxTe and Cd1-xMnxTe surface depending on treatment type,” Semiconductor Physics, 7 (1), 52-55 (2004).

[17] V.V. Diychuk, A.G. Voloshchuk, “Pourbaix diagram for the system Hg3In2Te6-H2O,” Science Bulletin of the ChNU., 606, 38-42 (2012).

[18] Naoto Takeno, Atlas of Eh-pH diagrams intercomparison of thermodynamic databases. Geological Survey of Japan Open File Report No.419, National Institute of Advanced Industrial Science and Technology, Research Center for Deep Geological Environments., 285. (2005).

[19] V.A. Riabin, M.A. Ostroumov,and T.F. Svit Thermodynamic properties of substances, Khimiya, Leningrad (1977).

[20] I. Kobasa I. Kondratyeva, and N. Husyak, “Spectral and photocatalytic properties of heterostructures with bisquinocyanine dye and ZnO, ZrO_2 and SiO_2,” Funct. Mater. Lett., 3 (4), 233-236 (2010) [doi: 10.1142/S1793604710001317].

[21] N.B. Gusiak, I.M. Kobasa, S.S. Kurek, “New dyes for dye-sensitized solar cells and photocatalysis. Verifying thermodynamic requirements for electron transfer,” Funct. Mater. Lett., 7 (3), 1450030 (2014).